Bubble Dissolution in Viscous Liquids in Simple Shear Flow

Moshe Favelukis, Zehev Tadmor, and Yeshayahu Talmon
Dept. of Chemical Engineering, Technion-Israel Institute of Technology, Haifa 32000, Israel

The dissolution of a gas bubble in a viscous Newtonian liquid in simple shear and creeping flow was studied experimentally. A simple theoretical model for bubble growth or dissolution at high Peclet numbers is also presented. The main result of the model shows that for high capillary numbers (slender bubbles) the dissolution or growth rate is proportional to the shear rate to the 3/8 power. The experimental work was carried out in a Couette apparatus. Air and carbon dioxide bubbles were injected into polymer liquids (low-molecular-weight polyisobutylenes) and photographed under shear. No "tip-streaming"was observed, and experimental results compared favorably with predictions of the simple model, based on a mechanism that combines diffusion and convection.

Introduction

Devolatilization (DV) is an elementary step in polymer processing in which volatile components (unreacted monomers, solvents, or water) are removed from the polymer after the polymerization reaction step. DV is carried out to improve the properties of the product, to meet environmental and health-related standards and for chemical recovery. Commercial DV involves heating the polymer and reducing the ambient pressure below the equilibrium partial pressure of the volatile component. This phenomenon, boiling, is accompanied by the formation of bubbles. The use of inert components such as nitrogen or steam that enhance foaming (bubbles) is often conducted in industry (Biesenberger, 1983). It is well known that DV by this mechanism is a very complicated process, often called BTDV (bubble transport devolatilization). According to this mechanism, the history of a bubble includes nucleation, movement in the melt, growth by molecular diffusion, coalescence and breakup, releasing its content to the ambient.

"Falling-strand" devolatilizers are often used in industry when the concentration of the volatile component is high (10–20%); however, at concentrations lower than 1% the separation is more difficult and expensive, and there is a need for special techniques. Usually in this concentration range, rotary machines based on screw extruders are used (Biesenberger, 1983). In this type of machinery the polymer melt is continuously sheared, and the rate of mass transfer may be influenced by the increased surface area (due to bubble deformation) and by external forced convection. Part of the advantage of using vented extruders was established experimentally by Tukachinsky et al. (1994).

Our previous work (Canedo et al., 1993) showed the effect of shearing on bubble deformation. Specifically, we investigated experimentally large deformation of gas bubbles in saturated viscous liquids in Couette flow. This article, a sequel to that, deals experimentally with the effect of shearing on mass transfer, specifically the dissolution of gas bubbles in viscous liquids in simple shear flow. Simple theoretical models for bubble dissolution (or growth) are also presented.

The interest in bubble dissolution stems from dissolution being the reverse of bubble growth, which takes place during a boiling DV process. Also the free air (bubbles) in the polymer melt may have an important role in determining the DV rate. Thus, air bubbles coming from the feed zone (for example, in a vented extruder) may act as nucleation sites. Moreover, bubble breakup in shear fields may be an efficient mechanism to produce new nuclei, provided these bubbles do not dissolve in the liquid. Hence the rate of dissolution of bubbles in shear fields or their life expectancy in the polymer melt may affect the DV process.

Theory

Bubble deformation

The deformation of a bubble (inviscid drop) in a Newtonian liquid in simple shear and creeping flow is governed by

---

Correspondence concerning this article should be addressed to Y. Talmon.

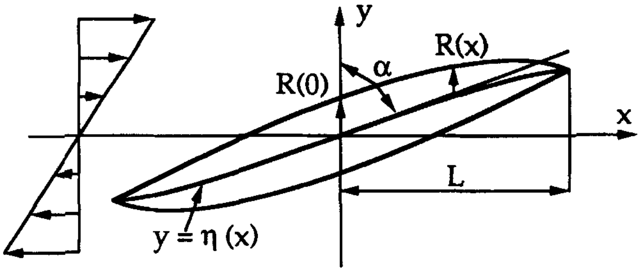

Figure 1. Deformation of a bubble in simple shear flow at $Ca \gg 1$.

$R(x)$—bubble's radius; $R(0)$—bubble's radius at bubble's center; L—half-length of the bubble; α—inclination angle; η-bubble's centerline.

a single dimensionless parameter, the capillary number (Ca), defined by

$$Ca = \frac{\mu \dot{\gamma} a}{\sigma}, \tag{1}$$

where μ is the liquid viscosity, $\dot{\gamma}$ is the constant shear rate of the unperturbed flow, a is the equivalent radius (radius of a sphere of equal volume), and σ is the surface tension. By checking the order of magnitude of this dimensionless number for typical DV processes, where bubbles are formed in polymer melts of large viscosities, it can be shown that $Ca \gg 1$. For small deformations, where $Ca \ll 1$, the bubble can be considered as a slightly perturbed sphere. However, at high values of the capillary number, $Ca \gg 1$, the theoretical analysis by Hinch and Acrivos (1980) predicts an elongated slender S-shaped bubble (Figure 1). Our previous work (Canedo et al., 1993) confirmed experimentally that theoretical model.

Bubble dissolution or growth

In a binary system of constant density and diffusion coefficient ($\mathfrak{D}$), and without reaction, a differential mass balance is given by

$$\frac{Dc}{Dt} = \mathfrak{D} \nabla^2 c, \tag{2}$$

where c is the molar concentration of the volatile solvent and t is the time. We restrict our model to dilute solutions, where the mass flux is small and does not influence the momentum transfer. We assume a uniform and constant concentration on the bubble surface (c_s) and far away from the bubble (c_∞). We further assume that the liquid at the bubble surface is in chemical equilibrium with the solvent vapor inside the bubble, so that we can apply Henry's law (Clift et al., 1978).

The relative magnitude of convection to diffusion is given by the Peclet number, defined as

$$Pe = \frac{\dot{\gamma} a^2}{\mathfrak{D}}. \tag{3}$$

For typical DV systems and for large (visible) bubbles, $Pe \gg 1$. In this case, the concentration boundary layer in the liquid, near the bubble's surface, is very thin (compared to the bubble's radius), and the concentration gradient normal to the surface is much greater than the concentration gradient parallel to the surface. When $Pe \gg 1$, the diffusion parallel to the surface can be neglected (Clift et al., 1978).

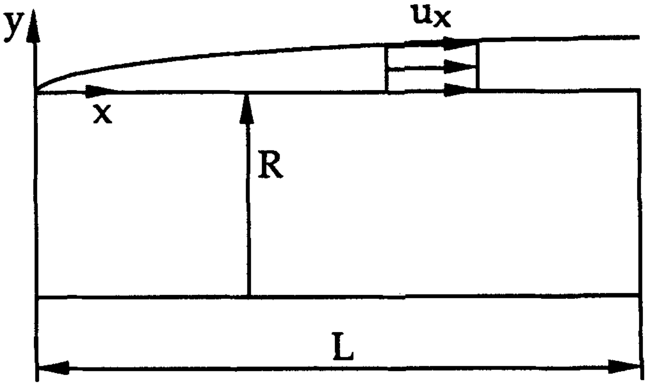

Figure 2. Part of a bubble and concentration boundary layer according to the simple model.

R—local bubble's radius; L—length of the mass-transfer path; u_x—velocity at the bubble's surface and in the concentration boundary layer.

Steady-state models

In this section we describe a simple steady-state model based on Higbie's theory (Bird et al., 1960), of mass transfer of the volatile solvent to or from the bubble in simple shear flow. Two cases are considered: (a) a slightly perturbed spherical bubble ($Ca \ll 1$); (b) a slender bubble ($Ca \gg 1$).

Let us assume the following: steady-state, creeping-flow, incompressible Newtonian fluids inside and outside the bubble, no buoyancy effects, no wall effects, isothermal conditions, and a thin concentration boundary layer. Figure 2 describes part of a bubble.

According to Bird et al. (1960), the average molar flux ($\bar{N}$) of the volatile component from the liquid to the bubble is

$$\bar{N} = 2(c_\infty - c_s)\sqrt{\frac{\mathfrak{D} u_x}{\pi L}}, \tag{4}$$

where u_x is the velocity component (assumed constant) in the x direction inside the concentration boundary layer (it is actually the velocity of the bubble surface); L is the length of the mass-transfer path. Equation 4 is a two-dimensional solution in Cartesian coordinates obtained by neglecting the convection term in the y direction of Eq. 2. The solutions with (Levich, 1962) or without (Bird et al., 1960) this term are on the same order of magnitude for the case of uniform creeping flow around a spherical bubble. We shall use this simplification, although in the present case the disturbed flow is three-dimensional.

It is also common to define the average molar flux as

$$\bar{N} = k(c_\infty - c_s), \tag{5}$$

where k is the average overall mass-transfer coefficient. Comparing Eqs. 4 and 5, the solution in terms of the Sherwood number, the ratio of the total mass transfer to the diffusional mass transfer, can be obtained:

$$Sh = \frac{ka}{\mathfrak{D}} \sim \left(\frac{a}{L}\right)^{1/2} \left(\frac{u_x a}{\mathfrak{D}}\right)^{1/2}. \tag{6}$$

We shall see later that this definition of the Sh number does not describe well the mass transfer, because it does not take into account the increase in the surface area as a consequence of shear. Therefore one defines a modified Sherwood number (Sh^*):

$$Sh^* = ShA^* = \frac{ka}{\mathfrak{D}} A^* \sim A^* \left(\frac{a}{L}\right)^{1/2} \left(\frac{u_x a}{\mathfrak{D}}\right)^{1/2} \tag{7}$$

where A^* is the dimensionless surface area (see Eqs. 11 or 15). Note that for a spherical bubble $Sh^* = Sh$.

For a nearly spherical bubble the order of magnitude of the surface velocity (u_x), the dimensionless radius (R^*), the dimensionless length of the mass-transfer path (L^*), and the dimensionless surface area (A^*) are

$$u_x \sim \dot{\gamma} a \tag{8}$$

$$R^* = \frac{R}{a} \sim 1 \tag{9}$$

$$L^* = \frac{L}{a} \sim 1 \tag{10}$$

$$A^* = \frac{A}{4\pi a^2} \sim 1, \tag{11}$$

while for the slender bubble we have (Hinch and Acrivos, 1980; Canedo et al., 1993)

$$u_x \sim \dot{\gamma} R \tag{12}$$

$$R^* = \frac{R}{a} \sim Ca^{-1/4} \tag{13}$$

$$L^* = \frac{L}{a} \sim Ca^{1/2} \tag{14}$$

$$A^* = \frac{A}{4\pi a^2} \sim Ca^{1/4}. \tag{15}$$

After substituting the previous parameters in Eq. 7, the final expressions for the steady-state solutions are: for a nearly spherical bubble ($Ca \ll 1$):

$$Sh^* \sim Pe^{1/2} \tag{16}$$

and for the slender bubble ($Ca \gg 1$):

$$Sh^* \sim Ca^{-1/8} Pe^{1/2}. \tag{17}$$

A specific problem arises in simple shear flow because the flow field is antisymmetric and not axisymmetric (as in the case of uniform flow). Let us examine the case of a spherical bubble in simple shear flow (Figure 3). The model assumes that the liquid entering the concentration boundary layer contains the solvent at the bulk concentration (c_∞). Near the two stagnation points one boundary layer starts but another one ends, and thus contaminates with solvent the beginning of the first one. However, for a spherical bubble (inviscid drop), contrary to a solid sphere, the streamlines in the x-y plane outside the bubble are completely open (Bartok and Mason, 1958). We can assume that the liquid entering the boundary layer does not contain solvent at exactly the bulk concentration. This may lead to a lower mass-transfer rate than predicted by the simple model.

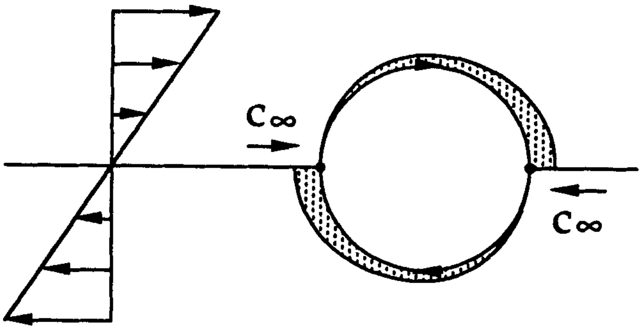

Figure 3. Concentration boundary layer around a spherical bubble in simple shear flow.

Quasi-steady-state models

For an expression for the rate of growth or dissolution, we assume ideal gas, uniform and constant pressure inside the bubble, only the volatile component in the bubble, isothermal conditions, and no buoyancy effects. The ideal gas equation is:

$$PV = nR_gT, \tag{18}$$

where P is the bubble's pressure, V is the bubble's volume, n is the number of moles inside the bubble, R_g is the universal gas constant, and T is the absolute temperature. Alternatively, we can write

$$n(t) = \frac{P}{R_gT} \frac{4}{3} \pi a^3(t). \tag{19}$$

By differentiation with respect to time, and dividing by the true surface area of the bubble, we get

$$\overline{N} = \frac{1}{A} \frac{dn}{dt} = \frac{P}{R_gT} \frac{1}{A^*} \frac{da}{dt}, \tag{20}$$

where $\overline{N}$ is the average molar flux of the volatile solvent, defined as positive for growth and negative for dissolution. The average molar flux was defined in Eq. 5 as follows:

$$\overline{N} = k\Delta c = k(c_\infty - c_s) = k\left(c_\infty - \frac{P}{H}\right), \tag{21}$$

where $\Delta c = c_\infty - c_S$ and H is Henry's constant (molar base).

From Eqs. 20 and 21, an expression for the growth or dissolution rate is obtained:

$$\frac{da}{dt} = FmSh^* \frac{\mathfrak{D}}{a}, \tag{22}$$

where *Fm* is a new dimensionless parameter, "the foaming number," similar to the Jakob number for mass transfer. *Fm* describes the part that thermodynamics plays in the growth or dissolution, as *Sh** describes the kinetic process:

$$Fm = \frac{R_g T \Delta c}{P}. \tag{23}$$

Good foaming is achieved by increasing *Fm*, since foaming is increased by working at high temperatures, small pressures, and large concentration differences.

In order to simplify and solve this type of problem, one of the most common assumptions is quasi-steady state. In this case we substitute the steady-state solution (for the *Sh** number) in the unsteady Eq. 22. It is often common to use this assumption when the growth or dissolution rate is small compared to the velocity of the liquid. Actually, it is very difficult to check this assumption without the exact solution of the problem.

Substituting expressions for *Sh** and *Fm* in Eq. 22 for the case of growing or dissolving bubbles in simple shear flow, we get: for a nearly spherical bubble ($Ca \ll 1$):

$$\frac{da}{dt} \sim \frac{R_g T \Delta c}{P} \mathfrak{D}^{1/2} \dot{\gamma}^{1/2}, \tag{24}$$

and for a slender bubble ($Ca \gg 1$):

$$\frac{da}{dt} \sim \frac{R_g T \Delta c}{P} \mathfrak{D}^{1/2} \left(\frac{\mu}{\sigma} \right)^{-1/8} a^{-1/8} \dot{\gamma}^{3/8}. \tag{25}$$

In the last equation the growth or dissolution rate hardly depends on the equivalent radius. But the most important result in designing rotary machines for DV is that it depends on the shear rate to the power of 3/8. Thus an increase in shear rate will increase the rate of mass transfer.

For the case of dissolution of gas bubbles in a liquid having no dissolved gas ($c_\infty = 0$), Eq. 25 reduces to

$$\frac{da}{dt} \sim -R_g T \frac{\mathfrak{D}^{1/2}}{H} \left(\frac{\mu}{\sigma} \right)^{-1/8} a^{-1/8} \dot{\gamma}^{3/8}. \tag{26}$$

The dissolution rate does not depend on the pressure and it is proportional to the solubility (which is inversely proportional to Henry's constant) and to the square root of the diffusion coefficient, a typical result for bubbles dissolving at $Pe \gg 1$. This last equation is compared with our experimental results.

Experimental Studies

The experimental system [a Couette flow apparatus (CFA)] and viscous Newtonian liquids (Chevron—low molecular weight polyisobutylenes, PB24 and PB32) were those used in our previous work (Canedo et al., 1993). A dissolution experiment at ambient pressure and room temperature was conducted as follows: the polymer was first degassed under high vacuum (~ 0.1 mmHg), moderate heating (~ 60°C), and constant stirring for a few days. Then the CFA was carefully filled with the polymer, avoiding the introduction of air bubbles. Either air or carbon dioxide bubbles were injected into the polymer. After shear began, the bubbles were photographed from the *X-Y* plane (as defined in Figure 1) at predetermined periods of time. We found that the most accurate and easy way to measure the equivalent radius during the experiment was to measure the length of the bubble and then calculate the equivalent radius using previous correlations for the dimensionless bubble half-length vs. the capillary number from deformation experiments. This procedure is acceptable because the equations in creeping flow are quasi-steady state. Thus, the time for the bubble to obtain its steady-state shape is negligible. At the beginning and the end of the experiment we compared the calculated equivalent radius with the real one. They were the same. This calculation, carried out for both air and CO_2 bubbles (using in the deformation correlations the surface tension of PB–air systems), proved also that the type of gas did not influence the surface tension. Neither bubble fracture nor breakup or bubble migration in the gap of the CFA were observed under shear. The upward movement of the bubble due to buoyancy was very slow. Furthermore, Taylor instabilities are not expected in the range of our experiments. The experimental system and technique are discussed in detail by Canedo et al. (1993) and Favelukis (1988).

Results and Discussion

Figure 4 shows photographs of dissolution of air bubbles in PB24 in the *X-Y* plane at ambient pressure and room temperature. Figure 4a shows a spherical bubble, having an initial radius of 1.2 mm, before shear has been applied. The same bubble, but deformed and at different times, is shown in Figures 4b–4d at a shear rate of 5.5 s^{-1}. A different bubble with the same initial radius is shown in Figure 4e, and in a deformed form in Figures 4f–4h at a shear rate of 16.6 s^{-1}. The length of the bubble is little affected at low shear rate, but decreases rapidly at the higher shear rate. Clearly, air bubbles dissolve slowly in polyisobutylene (about 30% decrease in the equivalent radius after 8 min). A linear correlation was found between the equivalent radius and the time (da/dt = const.).

Similar photographs are shown in Figure 5 for the CO_2/PB32 system, where the dissolution rate is much higher. Yet, here too we found the dissolution rate to be constant until the bubbles become very small, and the dissolution seems to almost cease. This last point needs further checking.

This work is summarized by Figure 6, which shows a log-log plot of the (constant) dissolution rate as a function of the shear rate for the three systems investigated. Clearly, there is a moderate increase in the dissolution rate with an increase in shear rate. The experimental slopes in the range 0.28–0.38 are very close to those predicted by the simple model (3/8).

Unfortunately, we did not have the diffusivities or solubilities of our investigated systems, and therefore a complete comparison of the experimental results with the simple model cannot be made. However, examining those two parameters

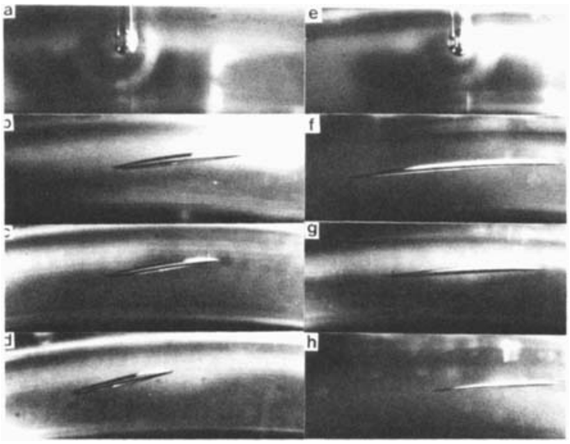

Figure 4. Dissolution of air bubbles in PB24 in the *X*-*Y* plane.

Left: $\dot{\gamma} = 5.5\ s^{-1}$, $T = 28.5°C$; (a) $t = 0$ min, $a = 1.2$ mm; (b) $t = 1.5$ min, $a = 1.14$ mm; (c) $t = 5.5$ min, $a = 0.98$ mm; (d) $t = 7.5$ min, $a = 0.92$ mm. Right: $\dot{\gamma} = 16.6\ s^{-1}$, $T = 30.0°C$; (e) $t = 0$ min, $a = 1.2$ mm; (f) $t = 1.1$ min, $a = 1.15$ mm; (g) $t = 5.1$ min, $a = 0.93$ mm; (h) $t = 8.0$ min, $a = 0.80$ mm.

(for other systems) we find that the square root of the diffusion coefficient of air and CO_2 are almost the same, but the solubility (inversely proportional to Henry's constant) of carbon dioxide is about one order of magnitude higher than the solubility of air. Therefore, for the same shear rate and according to the simple model, we would expect a much higher dissolution rate for CO_2 than air.

Several investigators have reported a phenomenon called "tip-streaming," in which small droplets are shed off from the main drop at the tip of the drop. This phenomenon was not observed in our experiments, even at large magnifications of the photographs. However, if "tip-streaming" were the main mechanism of dissolution, since we proved there are no differences in the surface tension between the two gases, one would not expect major differences between the dissolution rate of air and carbon dioxide bubbles. Hence, we conclude that the dissolution of bubbles in viscous liquids in simple shear flow is dominated by combined diffusion and convection and that the dissolution rate increases with an increase in shear rate.

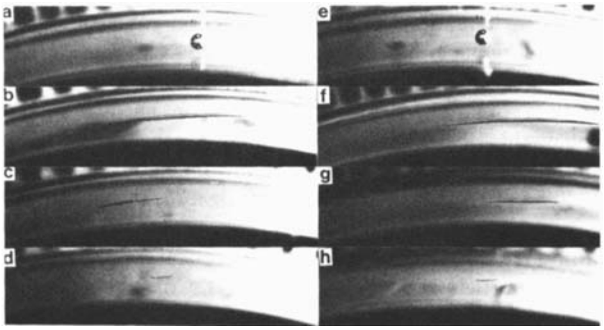

Figure 5. Dissolution of CO_2 bubbles in PB32 in the *X*-*Y* plane.

Left: $\dot{\gamma} = 6.6\ s^{-1}$, $T = 30.1°C$; (a) $t = 0$ min, $a = 1.4$ mm; (b) $t = 0.2$ min, $a = 1.33$ mm; (c) $t = 2.1$ min, $a = 0.79$ mm; (d) $t = 4.1$ min, $a = 0.34$ mm. Right: $\dot{\gamma} = 12.8\ s^{-1}$, $T = 30.0°C$; (e) $t = 0$ min, $a = 1.4$ mm; (f) $t = 0.3$ min, $a = 1.27$ mm; (g) $t = 1.8$ min, $a = 0.72$ mm; (h) $t = 4.0$ min, $a = 0.33$ mm.

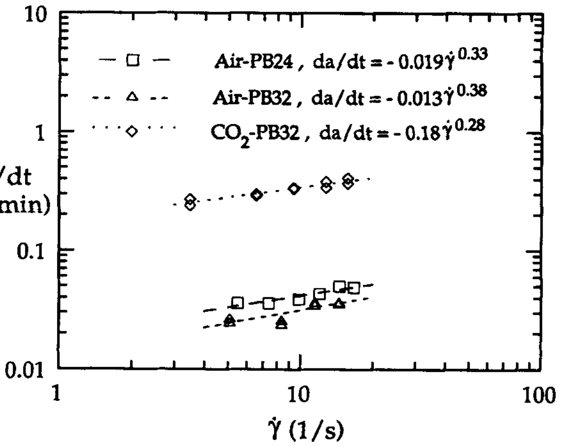

Figure 6. Dissolution rate of air and CO_2 bubbles in PB24 and PB32 as a function of the shear rate at 30°C and ambient pressure.

It is difficult to draw conclusions from our results, obtained in a well-controlled system for a single bubble, to the real commercial DV process. But these results indicate that higher mass-transfer rates are expected in rotary machines such as vented extruders, with an increase of shear rates at higher rotational speeds.

Acknowledgments

This research was supported in part by a grant from the National Council for Research and Development, Israel, and the Kernforschungsanlage, Jülich, Germany. We wish to thank Prof. A. Nir of the Technion and Prof. H. G. Fritz of the Institut für Kunstofftechnologie (IKT), Stuttgart, for useful discussions and productive cooperation in this project.

Literature Cited

Bartok, W., and S. G. Mason, "Particle Motions in Sheared Suspensions: VII. Internal Circulation in Fluids Droplets (Theoretical)," *J. Colloid. Sci.*, **13**, 293 (1958).

Biesenberger, J. A., ed., *Devolatilization of Polymers*, Hanser, Munich (1983).

Bird, R. B., W. E. Stewart, and E. N. Lightfoot, *Transport Phenomena*, Wiley, New York (1960).

Canedo, E. L., M. Favelukis, Z. Tadmor, and Y. Talmon, "An Experimental Study of Bubble Deformation in Viscous Liquids in Simple Shear Flow," *AIChE J.*, **39**, 553 (1993).

Clift, R., J. R. Grace, and M. E. Weber, *Bubbles, Drops and Particles*, Academic Press, New York (1978).

Favelukis, M., "Dissolution of Gas Bubbles in Viscous Shear Flows," MSc Thesis, Dept. of Chemical Engineering, Technion-Israel Inst. of Technol. Haifa (1988).

Hinch, E. J., and A. Acrivos, "Long Slender Drops in a Simple Shear Flow," *J. Fluid Mech.*, **98**, 305 (1980).

Levich, V. G., *Physicochemical Hydrodynamics*, Prentice-Hall, Englewood Cliffs, NJ (1962).

Tukachinsky, A., Y. Talmon, and Z. Tadmor, "Foam-Enhanced Devolatilization of Polystyrene Melt in a Vented Extruder," *AIChE J.*, **40**, 670 (1994).

Manuscript received June 20, 1994, and revision received Nov. 29, 1994.